NeuroImage: Clinical 14 (2017) 518–529

Contents lists available at ScienceDirect

NeuroImage: Clinical

journal homepage: www.elsevier.com/locate/ynicl

Parietal operculum and motor cortex activities predict motor recovery in moderate to severe stroke

Firdaus Fabrice Hannanu[a,b], Thomas A. Zeffiro[b,c], Laurent Lamalle[a,d,e,f], Olivier Heck[g,h], Félix Renard[i], Antoine Thuriot[i,k], Alexandre Krainik[a,d,e,f,g,h], Marc Hommel[b,i,j], Olivier Detante[b,h,k], Assia Jaillard[a,b,i,*], on behalf of the ISIS-HERMES Study Group

K. Garambois[1], M. Barbieux-Guillot[2], I. Favre-Wiki[2], S. Grand[3], J.F. Le Bas[4], A. Moisan[5], M.J. Richard[6], F. De Fraipont[6], J. Gere[7], S. Marcel[7], W. Vadot[8], G. Rodier[8], D. Perennou[9], A. Chrispin[9], P. Davoine[9], B. Naegele[2], P. Antoine[2], I. Tropres[10], F. Renard[11]

[1] Stroke Unit Centre Hospitalier UniversitaireGrenoble Alpes [CHUGA], France
[2] Stroke Unit CHUGA, France
[3] Neuroradiology CHUGA, France
[4] Neuroradiologie CHUGA, France
[5] Unité Mixte de Thérapie Cellulaire [UMTC] CHUGA, France
[6] UMTC, France
[7] Stroke Unit, CH Chambéry, France
[8] Stroke Unit, CH Annecy, France
[9] Rehabilitation Unit CHUGA, France
[10] IRMaGe UGA, France
[11] AGEIS-UGA, France

[a] Unité IRM 3T-Recherche- UMS IRMaGe – Centre Hospitalier Universitaire (CHU) Grenoble Alpes, France
[b] Laboratoire MATICE - Pôle Recherche – CHU Grenoble-Alpes, France
[c] Neurometrika, Potomac, MD, United States
[d] IRMaGe - Inserm US-017, France
[e] IRMaGe - CNRS UMS-3552, France
[f] IRMaGe - Université Grenoble-Alpes -, France
[g] Neuroradiologie et IRM-Centre Hospitalier Universitaire Grenoble-Alpes, France
[h] Grenoble Institut des Neurosciences (GIN) Inserm U836-UJF-CEA-CHU, France
[i] AGEIS, EA-UGA 7407 Université Grenoble Alpes, France
[j] Clinatec - CHU Grenoble-Alpes, France
[k] Unité neurovasculaire - CHU Grenoble-Alpes, France

ARTICLE INFO

Article history:
Received 9 November 2016
Received in revised form 9 January 2017
Accepted 22 January 2017
Available online 26 January 2017

ABSTRACT

While motor recovery following mild stroke has been extensively studied with neuroimaging, mechanisms of recovery after moderate to severe strokes of the types that are often the focus for novel restorative therapies remain obscure. We used fMRI to: 1) characterize reorganization occurring after moderate to severe subacute stroke, 2) identify brain regions associated with motor recovery and 3) to test whether brain activity associated with passive movement measured in the subacute period could predict motor outcome six months later.

Because many patients with large strokes involving sensorimotor regions cannot engage in voluntary movement, we used passive flexion-extension of the paretic wrist to compare 21 patients with subacute ischemic stroke to 24 healthy controls one month after stroke. Clinical motor outcome was assessed with Fugl-Meyer motor scores (motor-FMS) six months later. Multiple regression, with predictors including baseline (one-month) motor-FMS and sensorimotor network regional activity (ROI) measures, was used to determine optimal variable selection for motor outcome prediction. Sensorimotor network ROIs were derived from a meta-analysis of arm voluntary movement tasks. Bootstrapping with 1000 replications was used for internal model validation.

During passive movement, both control and patient groups exhibited activity increases in multiple bilateral sensorimotor network regions, including the primary motor (MI), premotor and supplementary motor areas (SMA),

* Corresponding author at: Unité IRM 3T Recherche - CHU Grenoble-Alpes - CS 10217, 38043 Grenoble, France.
E-mail addresses: Assia.Jaillard@ujf-grenoble.fr, assia.jaillard@gmail.com (A. Jaillard).

http://dx.doi.org/10.1016/j.nicl.2017.01.023

cerebellar cortex, putamen, thalamus, insula, Brodmann area (BA) 44 and parietal operculum (OP1-OP4). Compared to controls, patients showed: 1) lower task-related activity in ipsilesional MI, SMA and contralesional cerebellum (lobules V-VI) and 2) higher activity in contralesional MI, superior temporal gyrus and OP1-OP4. Using multiple regression, we found that the combination of baseline motor-FMS, activity in ipsilesional MI (BA4a), putamen and ipsilesional OP1 predicted motor outcome measured 6 months later (adjusted-$R^2 = 0.85$; bootstrap $p < 0.001$). Baseline motor-FMS alone predicted only 54% of the variance. When baseline motor-FMS was removed, the combination of increased activity in ipsilesional MI-BA4a, ipsilesional thalamus, contralesional mid-cingulum, contralesional OP4 and decreased activity in ipsilesional OP1, predicted better motor outcome (djusted-$R^2 = 0.96$; bootstrap $p < 0.001$).

In subacute stroke, fMRI brain activity related to passive movement measured in a sensorimotor network defined by activity during voluntary movement predicted motor recovery better than baseline motor-FMS alone. Furthermore, fMRI sensorimotor network activity measures considered alone allowed excellent clinical recovery prediction and may provide reliable biomarkers for assessing new therapies in clinical trial contexts. Our findings suggest that neural reorganization related to motor recovery from moderate to severe stroke results from balanced changes in ipsilesional MI (BA4a) and a set of phylogenetically more archaic sensorimotor regions in the ventral sensorimotor trend, in which OP1 and OP4 processes may complement the ipsilesional dorsal motor cortex in achieving compensatory sensorimotor recovery.

1. Introduction

Until recently, few biomarkers have effectively predicted therapeutic response or recovery following stroke, especially when measured in the acute or subacute phases of the disease (Burke Quinlan et al., 2015). Current clinical tools, such as Fugl-Meyer Assessment of Sensorimotor Recovery after Stroke [motor-FMS] (Sullivan et al., 2011), have limitations related to their subjective and qualitative nature. Therefore, discovery of more objective, quantitative, and efficiently acquired MRI biomarkers that can be collected at the time of diagnosis, will facilitate prediction of motor recovery in both clinical and research contexts (Bhatt et al., 2016; Burke et al., 2014; Wang et al., 2011).

Functional magnetic resonance imaging (fMRI) measures changes in neural activity with good reliability, making it a promising candidate for predicting stroke recovery (Gountouna et al., 2010; Kristo et al., 2014; Sun et al., 2013). The role of fMRI task-related sensorimotor activity in predicting stroke outcome has been reported using a range of methods and experimental designs (Favre et al., 2014; Rehme et al., 2012). More specifically, activity in primary motor cortex [MI] and supplementary motor area [SMA] were associated with good outcome in a recent meta-analysis of 24 studies using movement tasks (Favre et al., 2014). In addition, evidence that multiple sensorimotor regions can predict recovery, including dorsal premotor cortex [dPMC] (Johansen-Berg et al., 2002; Rehme et al., 2011), contralesional cerebellum (Rehme et al., 2015; Small et al., 2002; Ward et al., 2003), parietal cortex (Marshall et al., 2009), contralesional MI (Calautti et al., 2007; Rehme et al., 2011; Werhahn et al., 2003), and insula (Carey et al., 2005; Loubinoux et al., 2007) suggests that a spatially distributed collection of sensorimotor network regions is involved in neural reorganization and influences motor recovery after stroke. From a pathophysiological perspective, while the complete recovery typically observed in patients with mild stroke is associated with the restoration of a typical motor activity pattern (Loubinoux et al., 2007), the pattern observed in patients with more severe stroke showing limited recovery, is characterized by recruitment of additional regions, suggesting the involvement of compensatory mechanisms beyond those typically engaged in voluntary movement (Carey et al., 2006). Nevertheless, neural reorganization following large strokes has not been extensively explored, even though patients with more severe deficits are often the principal focus of new therapies.

As most severely affected stroke patients cannot easily produce voluntary hand movements, it is possible that brain activity measures related to passive limb movement could be more useful outcome predictors in treatment studies. In healthy subjects, passive movement causes modulation in both the intensity and extent of motor system activity in a pattern similar to that observed during voluntary movement (Blatow et al., 2011; Loubinoux et al., 2001; Tombari et al., 2004; Weiller et al., 1996). Moreover, passive tasks may have higher reproducibility because of lower associated neural activity variability related to the patient's degree of motor impairment, range and speed of motion, and required effort. Test-retest reproducibility studies of both active and passive limb movements in healthy subjects and stroke patients have shown good reliability both within and between sessions (Gountouna et al., 2010; Jaillard et al., 2005; Loubinoux et al., 2001; Quiton et al., 2014).

The first aim of this study was to characterize functional reorganization occurring after moderate to severe stroke. The second aim was to identify the specific sensorimotor network regions associated with concurrent and future motor performance. The third aim explored whether a regression model incorporating predictors obtained from sensorimotor network region measures collected in the subacute period, could predict motor outcome six months later, and thus serve as an aggregate biomarker of recovery.

For the study we used a passive wrist flexion extension [passive-FE] task to investigate patients with fMRI one month after moderate to severe stroke, comparing the observed passive-FE-related activity in stroke patients and healthy controls. Then, we investigated whether one month sensorimotor fMRI activity, lesion volume and corticospinal tract (CST) damage were associated with clinical scores measured concurrently and six months later. Finally, we used multivariable regression to assess whether particular sets of regional fMRI activity measures could predict motor outcome, specifically the six-month motor-FMS. In this process, lesion volume, CST damage extent, lesion side, sex and age were introduced as additional predictors in the multivariable predictive model. To test whether fMRI measures could predict motor recovery better than baseline clinical measures alone or in combination, we first entered the subacute period motor-FMS in the model and then introduced additional fMRI predictors. Then, the baseline motor-FMS was removed from the model to determine whether fMRI measures alone can be used as biomarkers of motor recovery. The findings are discussed in the context of a theoretical perspective in which both phylogenetically newer and older parts of the sensorimotor system change activity during the recovery process (Pandya, 2015 #985).

2. Materials and methods

2.1. Participants

Thirty-one stroke patients (mean age 52 ± 10 years; 20 males; 17 left lesions) admitted to the University Hospital of Grenoble Stroke Unit were consecutively enrolled as a part of the ISIS (Intravenous

Stem cells after Ischemic Stroke) and HERMES (HEuristic value of multimodal MRI to assess MEsenchymal stem cell therapy in Stroke) studies. The protocol for the ISIS-HERMES study received approval by our Institutional Review Board (Grenoble CPP), and informed consent was obtained from all participants. Patients were studied using fMRI at inclusion, one month after stroke and before intravenous autologous stem-cell treatment. They received standard medical care and were admitted to a stroke rehabilitation center where they received standard physical and occupational therapy. The study inclusion criteria were: right or left ischemic stroke within the internal carotid artery territory, neurological deficits persisting one month post-stroke (NIHSS = 7–23) and willingness to participate. Patients with neurological or psychiatric disease were excluded. Further study details are provided at the NCT-clinical trials website: https://clinicaltrials.gov/ct2/show/NCT00875654?term=ISIS+stroke+stem+cells&rank=1.

In addition, patients with claustrophobia, persistent carotid artery occlusion or severe wrist spasticity were not included in the fMRI study. Out of 31 patients enrolled, 21 underwent the fMRI protocol (Fig. 1). While only four patients could execute active repetitive flexion-extension of the paretic wrist, paretic wrist passive movements could be performed in the 21 right handed patients, and was thus used to study hand movement related activity in a sensorimotor network previously defined by meta-analysis of activity related to voluntary movement (Favre et al., 2014 #128). Brain imaging and demographic and baseline data for the 21 patients are shown in Fig. 2, Table 1 and Table S1. Comparisons between participating and nonparticipating patients are shown in Table 2. Twenty-four healthy controls (mean age 51 ± 9 years; 15 males; 24 right-handed), with no history of neurological or psychiatric disease, were also studied. All patients underwent FMS assessment including functional, sensory, upper-limb, lower-limb scores. Combining upper and lower-limb subscores resulted in the aggregate motor-FMS (total 0–100 range, 100 for maximum performance) that was used as the main outcome measure. The Purdue Pegboard Test [PPT] (Rapin et al., 1966) was used to assess fine hand movement impairment; NIHSS (Brott et al., 1989) to classify baseline stroke severity as moderate (7–15 NIHSS range) or severe (16–24 NIHSS range). Independence was measured using the Barthel Index (Mahoney and Barthel, 1965), and the Modified Rankin Score (mRS) (Rankin, 1957). Behavioral assessment was performed by a stroke neurologist (neurological examination, NIHSS, Barthel, mRS) and physiotherapist (FMS, PPT), blind to treatment allocation at baseline (one month after stoke) and six months later. Stem-cell therapy was administered after baseline assessment at three different levels: no stem cells, a low dose and a high dose. In this paper our goal was not to study the effect of the treatment on motor recovery but to test if fMRI activity could predict motor outcome, independently of any treatment effects. Therefore, to adjust for treatment, we entered treatment (with 3 levels) as a nuisance variable at first. Treatment effects on recovery and its relation to fMRI measures of sensorimotor network activity are explored in another manuscript in preparation.

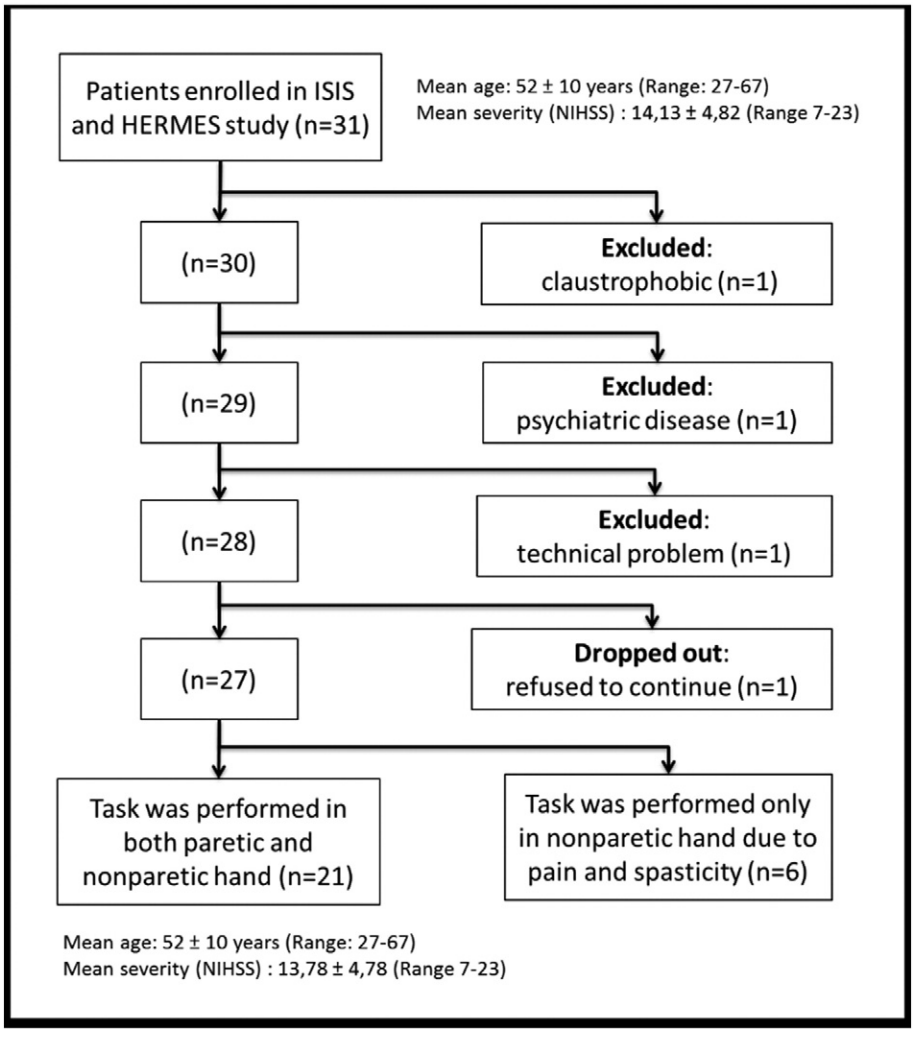

Fig. 1. Inclusion flow chart.

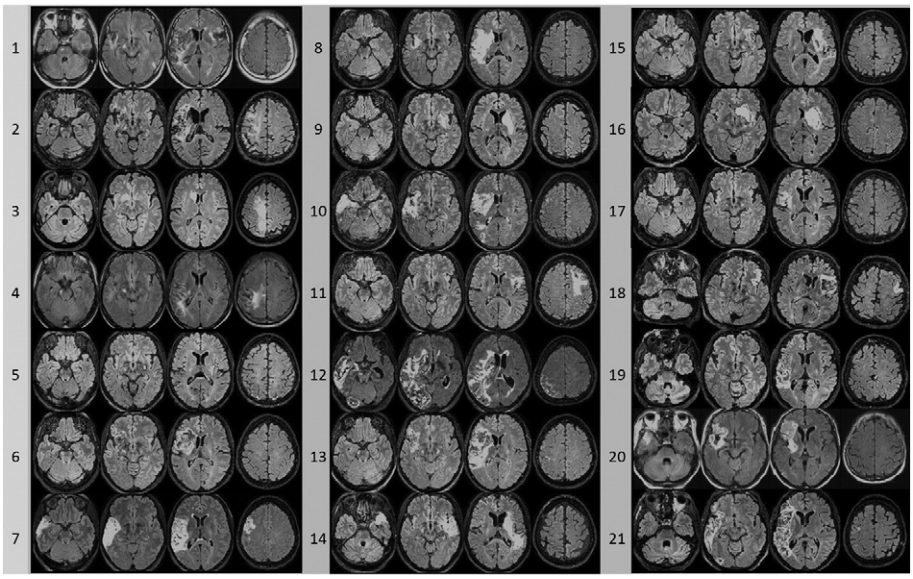

Fig. 2. Four axial slices representative showing stroke lesion extent in 21 patients (FLAIR images).

2.2. Image acquisition

An MRI system (Achieva 3.0T TX, Philips, NL.) at the IRMaGe MRI facility (Grenoble, France) with a 32 channel head coil was used. Echo planar images (EPI) were acquired during two sessions (113 EPI volumes per session) using the following parameters: TR 3 s, TE 30 ms, voxels 2.5 mm^3. High resolution (1 mm^3) structural images were acquired including sagittal T_1-weighted (TR 9.9 ms, TE 4.6 ms, flip angle 8°, TI 920 ms, intershot time 1792 ms) and 3D-FLAIR (TR 8 s, TE 342 ms). In addition, 60 direction diffusion imaging was used to obtain estimates of CST injury extent (Supplementary methods IA).

Passive-FE was studied for the paretic hand in patients and the matched hand in controls, with alternating 20 s epochs of 1 Hz 45° passive wrist flexion and extension and rest during 8 cycles (total time 5 min 40 s per hand). Movement rate has strong effects on task-related activity in sensorimotor network regions (Agnew et al., 2004). Since the presence of spasticity can affect both the velocity and range of passive movements in severe patients (Lindberg et al., 2009), we standardized the wrist movement task procedure. During the experiment, a white dot that could be seen by the examiner inside the room was flashed at 1 Hz on a screen. The examiner administered visually-cued passive flexion extension of the patient's wrist at 1 Hz over the range of 40°. A small supporting board strapped to the subject's hand was used to constrain the passive movements over a range of 40° (horizontal position to a maximum of 40°). All subjects were instructed to remain still and relaxed during the scan. While care was taken to observe mirror movements of the opposite hand or foot, none were observed.

Table 1
Baseline stroke features in the 21 patients.

N	Age	Sex	Lesion side	ART	Volume cm^3	Infarct arterial territory	Artery occlusion	Thrombolysis	Stroke diagnosis and related risk factors
1	46	M	L	24	115	MCA	No	tpa	Persistent foramen ovale
2	51	M	L	8	97	ICA	No	tpa	ICA dissection
3	38	F	L	2	47	ACA + superf MCA	No	No	ICA dissection; migraine
4	53	M	L	24	181	MCA	No	No	AF
5	50	M	R	0	19	Deep MCA	No	tpa	Hypertension; dyslipidemia
6	60	F	L	23	119	ICA	No	No	ICA stenosis (50%)
7	48	F	L	20	123	Superf MCA	No	No	Oral contraceptive; tobacco
8	59	M	L	23	73	MCA	No	No	Hypertension; dyslipidemia
9	57	M	R	0	36	MCA	No	No	Hypertension; tobacco
10	31	M	L	16	101	MCA	No	tpa	Tobacco; alcohol
11	45	M	R	0	60	Superf MCA	No	No	Tobacco
12	64	M	L	24	227	ICA	Yes	No	ICA occlusion (diabetes, dyslipidemia; tobacco)
13	41	F	L	14	112	MCA	No	tpa	ICA occlusion (dissection); oral contraceptive
14	52	M	R	0	83	MCA	No	tpa	ICA dissection
15	59	F	R	0	52	MCA	No	tpa	AF
16	42	F	R	0	55	MCA	No	tpa	Oral contraceptive
17	59	M	L	8	43	MCA	No	No	Atheroma (dyslipidemia; tobacco, alcohol)
18	65	M	L	10	72	MCA	No	No	AF; hypertension; dyslipidemia; tobacco
19	57	M	L	13	33	Superf MCA	No	tpa	ICA dissection; hypertension
20	62	M	L	5	70	MCA	No	tpa	Hypertension; dyslipidemia
21	67	M	L	26	150	MCA	No	no	Hypertension; sleep apnea syndrome
Total or mean (SD)	52.7 (9.6)	6 F	6 R	16.0 (8.0)	88.4 (52.6)	3 ICA/18 MCA	1 ICA occlusion	10 tpa	6 hypertension/4 ICA dissection/3 AF

M indicates male, F female, L left, R Right, Superf MCA superficial middle cerebral artery, ICA indicates internal carotid artery; AF atrial fibrillation, ART aphasia rapid test; higher score indicates severity. Artery occlusion indicates Artery occlusion at admission time. There was no persistent carotid artery occlusion at the time of the fMRI session.

Table 2
Comparisons of patients characteristics from the fMRI study (N = 21) and the non-fMRI group (N = 9).

Variables	fMRI patients (N = 21)		non fMRI patients (N = 9)		*t*-Test	Kruskal Wallis test
	Mean	SD	Mean	SD	p value	Asymp. Sig.
Age	52.67	9.63	48.89	12.30	0.37	0.48
Lesion volume [cc]	119.08	80.46	158.08	97.46	0.26	0.38
NIHSS V2	13.86	4.90	15.13	5.06	0.54	0.51
Barthel V2	47.14	33.15	36.88	32.06	0.46	0.39
ART V2	16.00	8.02	18.20	8.44	0.61	0.43
Rankin V2	3.67	0.58	4.13	0.35	0.05	0.04
mFMS V2	39.76	30.59	26.63	19.26	0.27	0.41
NIHSS V6	8.10	3.99	11.33	6.36	0.10	0.24
Barthel V6	85.95	20.10	68.75	37.58	0.12	0.32
ART V6	11.36	8.64	15.83	10.78	0.34	0.28
Rankin V6	2.81	0.60	3.33	0.50	0.03	0.03
mFMS V6	54.29	29.33	36.63	28.49	0.13	0.09
Categories	Cases		Cases			Chi-squared
Lesion side	6R:15L		3R:6L			0.56
Gender	15M:3F		6M:3F			0.56
Treatment	10;07;04		04;00;05			0.26

V2 indicates inclusion visit at baseline one month post-stroke; V6, Six month follow-up visit; ART = aphasia rapid test; mFMS = motor Fugl-Meyer subscore (max = 100). Treatment (no CSM; low doses; high doses).

2.3. Image preprocessing

Lesion volumes were determined by manual delineation of FLAIR images (Kuhn et al., 1989) and then used to mask T1-weighted images before preprocessing, including spatial normalization and realignment. Images from patients with right sided lesions were flipped about the y axis so that all lesions were on the left for analysis. Data preprocessing, performed using Statistical Parametric Mapping (SPM12: http://www.fil.ion.ucl.ac.uk/spm), is summarized in Fig. S2.

2.4. Quality assurance

Following visual inspection for spatial artifacts, EPI time series were checked for temporal artifacts and realigned. Intensity outliers were detected using ART (https://www.nitrc.org/projects/artifact_detect), with an interscan movement threshold of 1 mm, and a global interscan signal intensity threshold of 3 SD relative to the session mean.

2.5. Processing

First level voxel-wise analysis was performed using a general linear model including passive movement condition timing, motion outliers, head motion estimate regressors and a high-pass (128 Hz) temporal filter. The task regressors were convolved with a canonical HRF. Contrasts of the wrist movement-related parameter estimates were generated for subsequent group analysis.

Second level voxel-wise group analysis was performed for both control and patient groups using one-sample *t*-tests. The controls' matched hand was compared to the patients' paretic hand using a two-sample *t*-test. To assess the associations between neural activity and the clinical scores at one and six months post-stroke, the motor-FMS at one and at six months were introduced as covariates in separate one-sample *t*-tests. Lesion volume, CST damage, age and sex were then introduced as covariates in the one-sample *t*-tests, but removed from subsequent analysis as they had no significant effects. To allow visualization of the pattern of task-related activity effect sizes in the two groups, images are shown using a critical threshold of $p < 0.001$, uncorrected for multiple tests.

2.6. Sensorimotor network ROI analysis

As our goal was to determine if passive movement-related activity measured in regions typically active during voluntary movement could predict sensorimotor recovery, we selected *a priori* ROIs derived from a previous meta-analysis of upper-limb voluntary movement studies in 119 healthy subjects (Favre et al., 2014), previously reported as part of the sensorimotor network. For additional reviews see (Doyon et al., 2003; Eickhoff et al., 2010; Favre et al., 2014; Pandya, 2015). From these ROIs, we selected 17 right and 17 left ROIs including MI-4a, MI-4p, ventral PMC (vPMC), dorsal PMC (dPMC), SMA, SI-1, SI-3b, OP1/SII, OP4, midcingulate cortex (MCC), inferior frontal gyrus 'pars opercularis' (BA44), insula, putamen, thalamus and cerebellar lobules V, VI, VIIIa. ROIs were extracted from the SPM Anatomy Toolbox (Eickhoff et al., 2007) and from the AAL atlas (Tzourio-Mazoyer et al., 2002). Details are described in Supplementary data (Methods-IB). This procedure led to a set of 34 ipsilesional and contralesional ROIs spanning the voluntary limb movement network (Table 3). Using these ROIs, we assessed the relationship between passive-FE related brain activity in the ROIs and clinical scores with Pearson bivariate correlations computed between peak ROI Cohen's d effect sizes and the clinical scores.

2.7. Motor outcome prediction model

Sequential, hierarchical multiple regression was then used to identify the best model predicting motor outcome on the basis of clinical and passive movement-related MRI measures collected in the subacute period. The dependent variable was the main motor outcome measure, the six-month follow-up motor-FMS. First, we tested whether fMRI measures add additional predictive information compared to simple clinical measures. Baseline (one-month) motor-FMS was the first covariate entered in the multivariable predictive model, while the structural and functional MRI data, including regional brain activity effect sizes, lesion volume, CST damage extent and lesion side, were introduced using a forward stepwise method. Second, we tested using a second model whether fMRI measures alone could predict motor. Of note, the sample studied was part of a stem cell treatment trial. To account for any effects of therapy on motor outcome, treatment, modeled as 3 levels, was entered into both models before introducing the other variables. Then, a forward stepwise method was used to determine the most

Table 3
Correlations between motor Fugl Meyer scores and MRI parameters.

MRI variables	Number	Motor Fugl Meyer scale correlations			
		Inclusion (1 month)		6 months	
		r	P	r	p
fMRI ROIs (effect size)					
Left MI-4a	1.	**0.573****	0.007	**0.681****	0.001
Right MI-4a	2.	**0.467***	0.033	**0.433***	0.050
Left MI-4p	3.	**0.504***	0.020	**0.565****	0.008
Right MI-4p	4.	0.215	0.350	0.191	0.406
Left dPMC - BA 6 (-40,-12,56) *mta-aal*	5.	**0.624****	0.002	**0.705****	0.000
Right dPMC - BA 6 (58,6,26) *mta-aal*	6.	**0.543***	0.011	**0.531***	0.013
Left vPMC - BA 6 (-40,-12,56) *mta-aal*	7.	0.300	0.187	0.246	0.283
Right vPMC - BA 6 (64,8,22) *mta-aal*	8.	0.313	0.167	0.274	0.23
Left SMA (aal)	9.	**0.523***	0.015	**0.650****	0.001
Right SMA (aal)	10.	**0.593****	0.005	**0.657****	0.001
Left MCC *aal*	11.	**0.552****	0.009	**0.499***	0.021
Right MCC *aal*	12.	0.352	0.117	0.344	0.127
Left SI-1	13.	**0.514***	0.017	**0.588****	0.005
Right SI-1	14.	**0.475***	0.030	**0.449***	0.041
Left SI-3b	15.	**0.462***	0.035	**0.509***	0.018
Right SI-3b	16.	0.403	0.070	0.455*	0.038
Left OP1 - SII	17.	0.145	0.530	0.105	0.650
Right OP1 -SII	18.	**0.470***	0.032	**0.549***	0.010
Left OP4	19.	0.206	0.370	0.061	0.792
Right OP4	20.	**0.579***	0.006	**0.551***	0.010
Right insula	21.	0.445	0.043	0.403	0.07
Left insula	22.	0.371	0.098	0.383	0.086
Right BA 44	23.	**0.457***	0.037	**0.451***	0.040
Left BA 44	24.	0.286	0.208	0.310	0.172
Left thalamus (-16,-16,0) *mta-aal*	25.	0.017	0.943	0.039	0.867
Right thalamus (14,14,2) *mta-aal*	26.	0.229	0.319	0.113	0.625
Left putamen (-28,2,0) *aal*	27.	0.291	0.200	0.350	0.120
Right putamen (26,2,0) *aal*	28.	0.087	0.708	−0.014	0.953
Left lobule V	29.	0.335	0.138	0.427	0.053
Right lobule V	30.	**0.546***	0.011	**0.689****	0.001
Left lobule VI	31.	**0.440***	0.046	**0.579****	0.006
Right lobule VI	32.	**0.493***	0.023	**0.584****	0.005
Left lobule VIIIa	33.	−0.099	0.668	0.254	0.267
Right lobule VIIIa	34.	−0.021	0.929	0.011	0.963
Structural parameters					
Lesion volume cm^3		−0.349	0.121	−0.289*	0.204
CST damage percent		**−0.567**	**0.007***	**−0.583***	**0.005**

MI indicates primary motor area, SI primary somatosensory cortex, PMC premotor cortex, SMA, the supplementary motor area, MCC indicates the MidCingulate Cortex, OP the parietal operculum, lobule cerebellar hemispheric lobule. CST indicates corticospinal tract.
The added '*aal*' indicates that the anatomical ROI was taken from the Automated_Anatomical_Labeling (AAL) atlas. Note that the other ROIs are provided by the SPM anatomical toolbox from the Juelich atlas.
The added '*mta-aal*' indicates the common overlap between the sensorimotor region activated during a hand motor task in the meta-analysis (Favre et al., 2014) (see link) and (1) the precentral gyrus from the AAL atlas (Tzourio-Mazoyer et al., 2002) to obtain distinct functional ROIs representing the hand area within the dorsolateral PMC and within the ventrolateral PMC; (2) the thalamus from the AAL atlas and the cluster located within the thalamus in the meta-analysis.
** Correlation is significant at the 0.01 level (2-tailed).
* Correlation is significant at the 0.05 level (2-tailed); parameters are in bold characters for significant correlations.

parsimonious model (probability of $F < 0.05$ for entry and <0.10 for removal). The adjusted R^2 was used to compare model fits. Model performance was studied with calibration and discrimination. Calibration, referring to the agreement between outcome and predicted values, was examined using a plot of adjusted predicted values *vs* observed values of the motor-FMS. Discrimination, a measure assessing prediction accuracy, was explored by examining a histogram of the standardized residuals. Violations of model assumptions were assessed using standardized residual plots. The Durbin–Watson statistic was used to detect the presence of autocorrelation in the residuals. The severity of predictor variable multicollinearity was estimated with the variance inflation factor (Kutner et al., 2004).

2.7.1. Internal validation

A limitation of multivariable linear regression based on adjusted R^2 is the possibility of model overfitting resulting from inclusion of too many predictor variables, as all of the experimental variance can ultimately be modeled with a large enough predictor set. Internal validation can reduce the probability of overfitting by indicating an upper limit to the expected performance of the model in different datasets. Thus, multiple regression was coupled with bootstrap resampling with 1000 replications to construct 95% confidence intervals and obtain unbiased estimates of prediction accuracy (Steyerberg et al., 2001).

Data analysis was performed using SPM12 and STATA-13 (http://www.stata.com/).

3. Results

The motor-FMS increased from 39.8 ± 30.6 at one month to 54.3 ± 29.3 at six months after stroke (Table 2). Most stroke lesions were large. All involved the middle cerebral artery territory and MI was partially damaged in four patients (Fig. 2). Patient characteristics, lesion volumes and clinical scores are presented in Tables 1, 2 and S1. No statistically significant group effects of age, sex or lesion volume on motor performance measures were detected. (Table S2).

3.1. Voxel-wise analysis of passive-FE task-related brain activity

We first examined voxel-wise models of task-related activity within and between groups. In controls, passive-FE was associated with expected strong bilateral activity increases across the sensorimotor network including contralateral MI-4a, 4p, SI, dPMC, SMA, and putamen, ipsilateral MI-4p, SI-3a, bilateral cerebellum (vermis, lobules V-VI-VIII), thalamus, OP1-OP4 and BA44. For the patients, passive-FE resulted in a spatially typical, but less intense, pattern of activity, including ipsilesional MI-4a, MI-4p, SI, dPMC, SMA, cerebellar lobule VI, bilateral

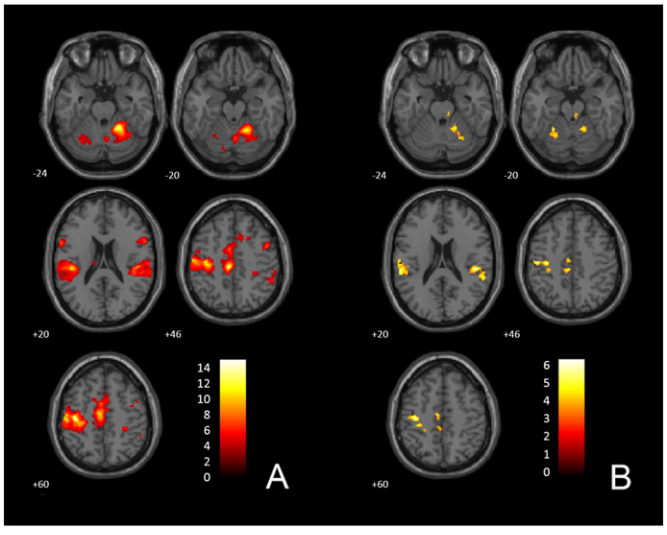

Fig. 3. T1-rendered montage of brain activity during passive movement in healthy controls and stroke patients in: (A) 24 healthy control and (B) 21 patients. Axial slices are shown for $z = -24, -20, 20, 46$ and 50 mm. An uncorrected threshold of $p < 0.001$ is used to allow visualization of the spatial distribution of activity and corresponding effect sizes. The color of the bar indicates the intensity of brain activity (t-statistic). The right hand is the referent hand for both controls and patients. The left hemisphere is represented on the left side of picture (neurologic convention). z MNI coordinates are indicated in the bottom left corner. Table S3 lists the peak coordinates and corresponding effect estimates.

OP1-OP4, contralesional cerebellar lobule V and pedunculopontine nucleus (Table S3; Fig. 3).

Comparing the control and patient groups, controls had greater activity in: ipsilesional MI-4p and SMA, and contralesional cerebellar lobule V. In controls, lower contralesional activity was seen in MI-4a, MI-4p, SI-3b, superior temporal gyrus and OP4 (Table S4; Fig. 4).

Concerning the relationship between passive-FE task-related brain activity and motor-FMS scores, we observed a positive association between the baseline motor-FMS and activity in bilateral dPMC, MI-4p, SMA, MCC and contralesional SI-3a, BA44 and cerebellar lobules V-VI. The outcome motor-FMS showed positive associations with activity in: ipsilesional dPMC, thalamus and contralesional SI-2, SMA, MCC, OP1-OP4, cerebellum V-VI (Table S5; Fig. S2).

3.2. ROI analysis of passive-FE task-related brain activity and motor performance

Next we examined associations among the set of the 34 left and right sensorimotor regions (Table 3 - bolded regions) and both concurrent and later motor performance measures. The concurrent and six-month follow-up motor-FMS were consistently related to activity in; (1) bilateral MI-4a, SI-1, dPMC, SMA and cerebellar lobule VI; (2) ipsilesional MI-4p, SI-3b, MCC; and (3) contralesional OP1, OP4, BA44, and cerebellar lobule V. CST injury extent, but not lesion volume was associated with baseline and six-month motor-FMS (Table 3). Bivariate correlations between individual ROI activity measures and NIHSS and mRankin scores at one and six months are reported in Table S6.

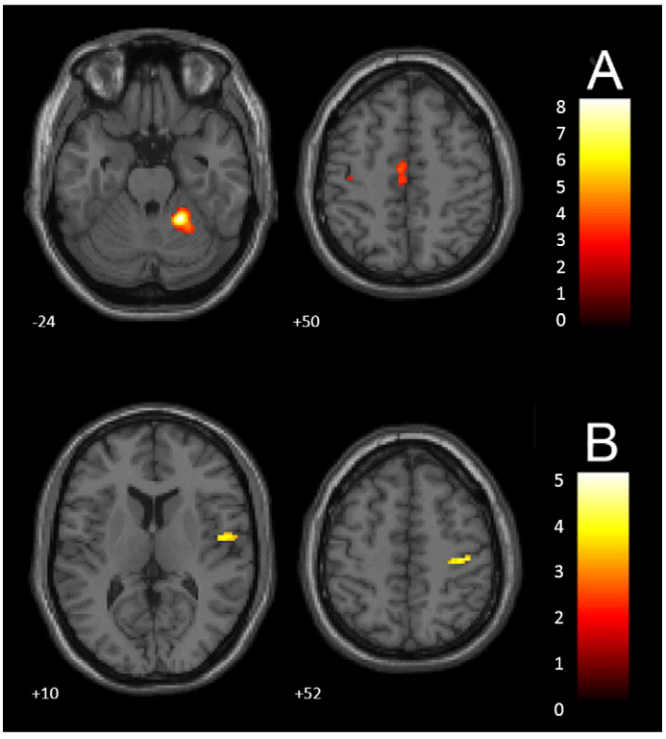

Fig. 4. T1-rendered montage of brain activations during passive movement for (A) Controls minus Patients comparison (z = −24, 50 mm) and reverse (B) Patients minus Controls, z = 10, 50 mm). Threshold is $p < 0.001$. The color of the bar indicates the intensity of brain activity (t-statistic). The right hand is the referent hand for controls and patients. The left hemisphere is represented on the left side of picture (neurologic convention). z MNI coordinates are indicated in the bottom left corner. See Table S4 for details.

3.3. Motor outcome prediction models

We then tested whether functional and structural measures could predict motor recovery using stepwise multivariable linear regression. Treatment status and baseline motor-FMS were first entered in the model while lesion volume, CST damage and task-related brain activity effect sizes from the sensorimotor ROIs were introduced using a stepwise approach. The most efficient model for predicting motor outcome, as judged by low variance inflation factor (VIF) for the predictors, high adjusted $R^2 = 0.87$, and the dispersion of the residuals, included, in addition to treatment status and baseline motor-FMS, ipsilesional MI-4a, putamen and OP1, (Tables 4&5, Fig. 5). Baseline motor-FMS alone accounted for 54% and fMRI predictors for 15% of the variance (Table 6).

The optimal model testing the predictive utility of fMRI measures, included, in addition to the treatment level: ipsilesional MI-4a, OP1 and thalamus, contralesional MCC and OP4, each accounting for 36%, 7%, 8%, 7%, and 19% of the variance, respectively. The model adjusted-R^2 was 0.96 (Tables 4&5, Fig. 5).

For both models, bootstrap analysis with 1000 repetitions verified the each model's stability and internal validity (Table 5). Coefficients and confidence intervals for each variable are shown in Table 5. Furthermore, Durbin and Watson statistics showed no evidence that the error terms were autocorrelated. The VIF indicates that variables were uncorrelated with the other predictor variables in the models. Observed outcome motor-FMS correlated with adjusted predicted values of outcome motor-FMS for both the clinical-fMRI model ($r = 0.89$, $p < 0.001$) and the fMRI model ($r = 0.97$, $p < 0.001$) (Fig. 6). Residuals were all below 2, indicating high accuracy for both models (Fig. S3).

4. Discussion

To explore neural reorganization after moderate to severe stroke and assess the utility of fMRI in predicting stroke recovery, our analysis strategy included: (1) using voxel-wise modeling to identify activity patterns associated with passive movement in both healthy participants and stroke patients, (2) using voxel-wise regression to compare differences between these groups in passive movement-related activity, (3) examining how ROI measures of subacute passive-FE activity are related to concurrent and later motor performance, and (4) assessing models predicting clinical recovery from aggregate regional fMRI and structural measures. We find that passive movement-related activity measured soon after stroke from a collection of regions associated with voluntary movement, can predict motor performance six months later. Some of these regions are located in the parietal operculum and may be part of a phylogenetically old system for motor control that may be important in supporting the motor recovery process.

4.1. Functional activity changes across the sensorimotor network in patients

Voluntary limb movement is typically associated with widespread, synchronous activity modulations in a spatially distributed, highly integrated network (Lin et al., 2009). Even so, with relatively rare exceptions (Rehme et al., 2015) most neuroimaging recovery studies utilize modeling strategies that incorporate isolated regional activity to explain recovery, while it is likely that considering aggregate influences from multiple regions may provide better predictive capabilities.

Passive wrist movement in the stroke group led to activity in the ipsilesional MI, SI, SMA, dPMC, cingulum, putamen, bilateral cerebellar lobules V-VI, thalamus and insula (Fig. 3), all areas frequently reported in stroke studies utilizing voluntary movement (Jang et al., 2004; Marshall et al., 2009; Rehme et al., 2011; Ward et al., 2003). Compared to healthy controls, our patients showed higher bilateral activity in OP1, a somatosensory region in the parietal operculum (Eickhoff et al., 2007), and lower activity in canonical motor regions, including ipsilesional MI, SMA and contralesional cerebellar lobules V-VI (Fig. 4), in agreement

Table 4
Coefficients of determination for predicting motor Fugl Meyer scale at 6 months follow-up based on baseline motor Fugl Meyer scale, treatment, and functional parameters (Model 1) and treatment and functional parameters (Model 2) using Linear regression and bootstrap with 1000 replications 2. Contribution of FMS without fMRI variables is 54%.

Model	R	R^2	Adjusted R^2	SE	Change statistics					Durbin Watson
					R^2 change	F change	df1	df2	Sig. F change	
1	0,949	0,900	0,867	10,694	0,150	7545	3	15	0,003	1838
2	0,985	0,969	0,956	6131	0,756	69,158	5	14	0,000	1929

with others (Carey et al., 2006; Loubinoux et al., 2003). However, in several previous studies employing voluntary movement (Wang et al., 2011; Ward et al., 2006), the stroke group exhibited higher activity in sensorimotor areas, presumably due to compensatory efforts to maintain the functional integrity of the network in the face of focal damage to its nodes or connections. The association of stroke with decreased regional activity could be related to two factors. First, our stroke sample has mostly large lesions, with a one-month baseline mean NIHSS = 13.78, indicating substantial clinical impairment. In contrast, patients from most previous stroke recovery studies were able to make hand movements and had smaller subcortical lesions. It is likely that the extent of sensorimotor network damage influences the aggregate level of task-related activity recorded (Carey et al., 2006). Second, passive movement is unlikely to engage the sorts of compensatory, effort-related processes associated with voluntary movement performed following focal damage to the sensorimotor network. As passive movement probes are not expected to be associated with higher effort by stroke patients, using them may provide a reliable means of assessing sensorimotor network function in the absence of compensatory influences.

4.2. Role of the contralesional motor network in recovery

Contralesional SI, MI, dPMC and SMA activity were consistently associated with both concurrent and future motor performance, with the dPMC also associated with neurological assessment and functional independence measures (Tables 2 and S6), suggesting that contralesional MI and premotor cortex activity may be associated with stroke recovery, in agreement with prior studies (Favre et al., 2014; Kantak et al., 2012; Loubinoux et al., 2007; Marshall et al., 2000). Nevertheless, the precise role of contralesional sensorimotor regions in recovery is still debated. On one hand, atypical interhemispheric balance with higher contralesional hemisphere activity can be associated with poor recovery (Calautti et al., 2007; Wiest et al., 2014), with impaired motor performance often attributed to disruption in inter-hemispheric inhibition, where an overactive contralesional area is believed to suppress activity in the lesioned hemisphere (Auriat et al., 2015). On the other hand, higher activity observed soon after severe stroke in contralesional primary motor and premotor cortices has been related to good recovery (Rehme et al., 2012). In large stroke lesions, where the ipsilesional hemisphere is too damaged to support complete recovery, additional compensatory mechanisms might involve contralesional motor areas, explaining response variability to rTMS in stroke (Auriat et al., 2015). Indeed, deleterious effects of contralesional motor cortex inhibition using rTMS have been observed following severe stroke (Bradnam et al., 2012).

Along these lines, we observed higher contralesional OP1, OP4, and BA44 activity in association with better motor performance at both times. Based on both architectonic and connectional anatomical evidence (Pandya, 2015), BA44, OP1 and OP4 are phylogenetically ancient sensorimotor regions, as compared to SI and MI (Pandya, 2015). The positive relationship observed between sensorimotor network activity in the contralesional hemisphere and clinical scores suggests that contralesional regions of both ancient and recent evolutionary origin in the sensorimotor network function as one system in supporting motor recovery, particularly when the compensatory capacity of the damaged hemisphere is overcome by large lesions.

4.3. After focal damage, passive-FE activity is associated with both concurrent and later motor performance

The voxel-wise modeling approach, examining associations between task-related activity and motor performance, showed results very similar to those seen in the between group comparison, demonstrating that bilateral sensorimotor network activity, including contributions from ipsilesional thalamus and MI, PMC, bilateral SMA, contralesional cerebellum V-VI, MI, and OP1-OP4, has both concurrent and predictive behavioral concomitants.

A complementary *a priori* ROI modeling approach, based on effect sizes observed in a set of regions identified by active voluntary

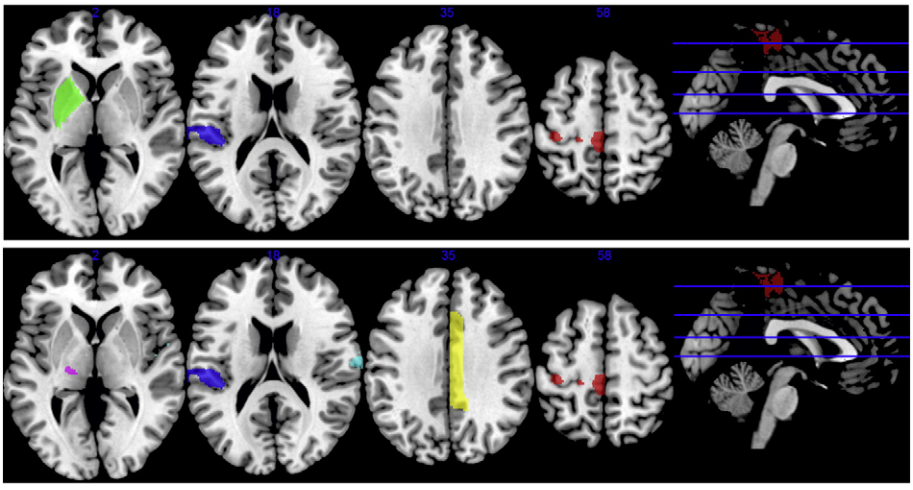

Fig. 5. Upper row: Predictive pattern for Model 1 including baseline motor-FMS including left putamen (green), OP1 (blue) and MI-4a (red). Lower row: Predictive pattern for Model 2 including - fMRI model- showing left OP1 (blue), and thalamus (pink), MI-4a (red), right anterior mid-cingulum (yellow) and OP4 (cyan). The left side indicates the lesioned hemisphere.

Table 5
Bootstrap for coefficients in Models 1 and 2.

Model	B	Bias	SE	Sig. (2-tailed)	95% confidence interval	
					Lower	Upper
Model 1						
(Constant)	−25,92	2,92	16,54	0,107	−49,50	10,75
Treatment	10,58	−0,33	4,18	0,036	0,73	17,26
Baseline motor-FMS	0,44	0,02	0,17	0,027	0,14	0,77
OP1-SII ipsilesional	−36,16	−1,62	16,58	0,045	−72,28	−5,34
Putamen ipsilesional	84,83	−6,97	34,51	0,040	6,82	136,04
Putamen ipsilesional	18,44	0,30	5,52	0,017	8,10	29,62
Model 2						
(Constant)	−25,34	0,69	7,32	0,014	−38,73	−9,20
Treatment	19,64	−0,21	2,30	0,001	14,96	24,00
OP1-SII ipsilesional	−39,77	−2,64	9,99	0,011	−61,56	−24,56
BA4a ipsilesional	17,62	0,49	2,68	0,004	14,17	24,14
Thalamus ipsilesional	79,02	−0,43	17,55	0,006	42,32	114,05
OP4-PV contralesional	134,23	0,45	27,08	0,004	77,85	186,21
MCC contralesional	184,76	−4,93	37,90	0,002	109,58	252,70

movement in healthy controls (Favre et al., 2014), also showed strong associations between motor-FMS scores and sensorimotor network regions in ipsilesional and contralesional hemispheres. When investigating global neurological assessment (NIHSS) and independence (mRankin score) as outcome measures, significant associations with better outcomes were associated with higher activity in contralesional MI, SI and dPMC for the mRS and ipsilesional MI, SI, dPMC, and SMA and contralesional MI, dPMC for NIHSS at 6 months. The bilateral dPMC and dorsal MI-4a, both parts of the dorsal sensorimotor stream in the precentral gyrus (Pandya, 2015 #1029), were consistently related to recovery, including neurological assessment and independence measures.

In the subacute stroke phase, ipsilesional MI, SI, MCC, bilateral SMA and contralesional cerebellar lobules V-VI, regions all involved in voluntary movement control, were correlated with both concurrent and future motor performance, consistent with previous studies (Tables 2-S6) (Bradnam et al., 2012; Calautti et al., 2007; Carey et al., 2005; Loubinoux et al., 2007; Marshall et al., 2000; Rehme et al., 2011; Tombari et al., 2004). These data support the assumption that passive wrist movement can be used to reliably identify the sensorimotor network typically engaged during active movement. In addition, some of these *a priori* ROIs including insula, BA44, OP1 and OP4, showed activity associated with both concurrent and future motor performance. Their role in the ventral sensorimotor stream is discussed further.

4.4. Regression models for predicting clinical outcome at six months

After adjusting for stem cell treatment level, the first multiple linear regression model had four predictors, baseline Fugl-Meyer and activity estimates from ipsilesional MI-4a, OP1, and putamen. Baseline Fugl-Meyer alone accounted for 54% of the variance, confirming the limited predictive capacity of clinical measures alone (Burke et al., 2014). Motor outcome adjusted for baseline motor-FMS, was predicted by higher activity in MI-4a and putamen, and lower activity in OP1, suggesting that an activity balance favoring the dorsal sensorimotor stream (MI-4a) relative to the ventral sensorimotor stream (OP1) promotes motor recovery. We also showed that fMRI measures combined with baseline motor-FMS was better than clinical assessment alone for motor outcome prediction, with fMRI accounting for 15% of the total variance and 50% (15/30) of the remaining variance. In the second model, built with only MRI measures, performance reached $R^2 = 96\%$, indicating that fMRI alone can predict motor outcome much better than clinical measures alone ($R^2 = 54\%$) or baseline-FMS and fMRI measures combined ($R^2 = 87\%$) (Table 6). Higher OP1 activity predicted worse outcome while higher ipsilesional MI-4a, MCC, premotor thalamus and contralesional OP4 activity indicated better outcome. The predictive capability of measures from sensorimotor system components with distinct phylogenetic origins suggests that mechanisms of recovery in moderate and severe stroke may differ from those reported in recovery from milder strokes. Implications of this finding are discussed below.

4.5. Role of the ipsilesional primary motor cortex, MI

MI-4a activity was the strongest individual predictor of recovery, accounting for 36% of the variance, confirming previous findings that MI activity, measured in acute through chronic periods, is typically associated with better recovery (Favre et al., 2014; Jaillard et al., 2005; Loubinoux et al., 2007; Rehme et al., 2015), although others have reported no effect (Marshall et al., 2009) or an association with worse outcome (Cramer et al., 2007). The reason why MI-4a was identified as a better recovery predictor than MI-4p could be related to associated damage to MI-4p in four patients and to the fact that the motor-FMS assesses motor performance of the upper and lower limbs, rather than digit dexterity that is more related to MI-4p (Jaillard et al., 2005). Furthermore, a supportive role in motor recovery has also been reported for MI-4, endorsing a vicarious function allowing complete recovery in four patients with stroke lesions restricted to MI-4p (Jaillard et al., 2005).

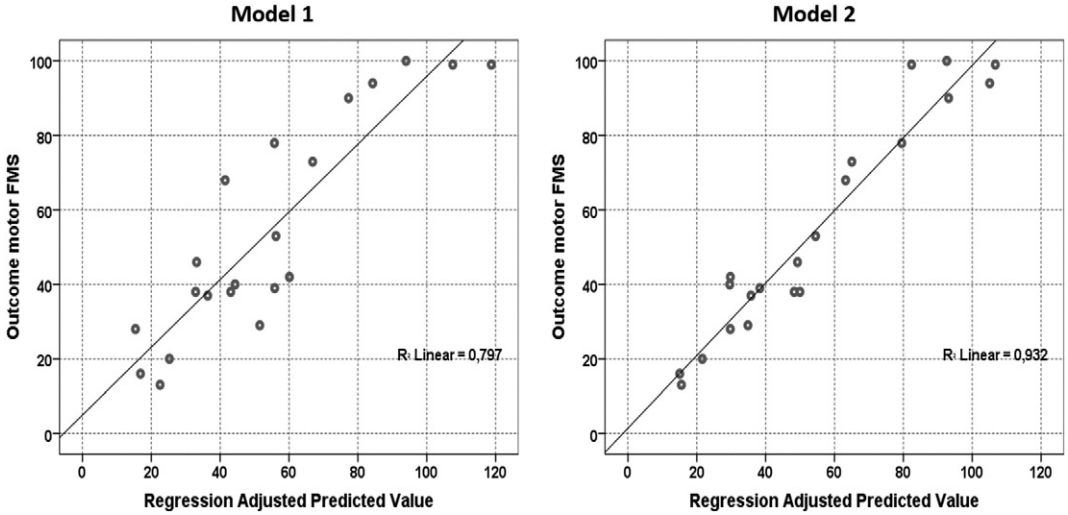

Fig. 6. Plot of predicted and adjusted motor-FMS values for Model 1 ($R^2 = 0.797$) and Model 2 ($R^2 = 0.932$).

Table 6
Coefficients of determination for predicting motor Fugl Meyer scale at 6 months follow-up based on clinical, structural, clinical + fMRI and fMRI measures ($p < 0.05$) after adjusting for stem cells treatment.

Models	Baseline mFMS	Structural MRI	functional MRI + baseline FMS	Functional MRI
Adjusted R^2	0.536	0.27	0.87	0.96

4.6. Role of the cortico-striato-thalamo-cortical sensorimotor loop

Our findings showed that the putamen, thalamus and MCC were predictors of good outcome, although accounting only for 5% of the variance in the combined clinical score-fMRI model and 15% in the fMRI model. The MCC includes the motor component of the cingulate gyrus and is associated with movement control, supported by its reciprocal connections with MI, its projections through the cortico-spinal tract and its identification in neuroimaging motor stroke studies (Carey et al., 2005; Tombari et al., 2004). Indeed, MCC participates in the control of voluntary movement, motor response preparation and motor learning (Cadoret and Smith, 1997; Vogt and Vogt, 2003). The putamen and thalamus are other key regions dedicated to motor learning (Doyon et al., 2009). For example, the putamen is active when a movement sequence of is well learned and its execution has become automatic (Doyon et al., 2009). The MCC, putamen and thalamus are all essential components of the cortico-striato-thalamo-cortical sensorimotor loop. Their role in motor recovery may be in restoring motor routines necessary for relearning skilled motor behavior (Doyon et al., 2003).

4.7. Role of the parietal operculum, part of the ventral sensorimotor system

We observed passive-FE effects in OP1 and OP4 in both healthy and stroke participants, and in contralesional OP1-OP4 comparing patients *versus* controls. OP1 and OP4 activity predicted motor outcome. OP1 and OP4 activity were also seen in a recent meta-analysis of voluntary limb movement studies in healthy participants (Favre et al., 2014). Human OP1 (Fig. 5), which occupies the caudal part of the parietal operculum (Eickhoff et al., 2007), corresponds to the second somatosensory representation (SII), first described in the monkey (Woosley, 1958). OP1 is densely connected to both somatosensory and motor areas (parietal cortex, thalamus, SI, MI, PMC, BA44), allowing it to serve an integrative role in sensorimotor processing. Neurons with attention and stimulus discrimination sensitivity have been described in monkey area SII, suggesting that OP1 may facilitate the incorporation of proprioceptive information in processes related to movement preparation and execution supporting stroke recovery.

We showed increased OP4 activity in patients compared to healthy controls, suggesting that OP4, monkey area PV lying in the rostral part of the parietal operculum, is involved in stroke recovery. Because of its strong connections to lateral PMC, OP4 may play a role in sensorimotor integration, potentially incorporating tactile and proprioceptive feedback into movement preparation and control of movement (Eickhoff et al., 2010). These results suggest that ventral and dorsal sensorimotor systems, originating from both proisocortex and isocortex (Pandya, 2015), and showing activity during voluntary movement, jointly contribute to sensorimotor recovery as a unitary system supporting optimal motor function.

From an evolutionary perspective, MCC, OP1/SII and OP4 are considered root areas that are associated with phylogenetically more ancient parts of the vertebrate pallium, compared to more recent core areas such as MI (Pandya, 2015). The thalamus and putamen, part of the diencephalon, are also phylogenetically older brain structures. Following stroke involving extensive damage to the motor network, the capacity to recover motor function through local reorganization may be limited, and essentially dependent on these archaic regions. Accordingly, high activity in the ventral sensorimotor network early after stroke may foretell the sort of poor recovery that would require specific therapeutic approaches.

Interestingly, OP1 and OP4 activity have not been frequently reported in previous recovery studies. One explanation is that these studies were limited to patients who could perform voluntary movement tasks and thus did not have severe movement deficits. In this circumstance, recruitment of the more ventral sensorimotor stream was not needed for behavioral compensation. The identification of OP1 as a recovery predictor, may reflect the passive nature of the task, as activation of OP1, a region integrating somatosensory information, is more likely when using passive tasks (Eickhoff et al., 2010). Alternatively, the present work may reflect the benefits of using higher spatial resolution and homogeneity in terms of MRI acquisition techniques, as the same high resolution protocol was used for all of our patients and controls, resulting in greater spatial accuracy.

4.8. Measures of structural volume and CST damage

Consistent with previous studies, CST lesion load (Burke Quinlan et al., 2015; Feng et al., 2015; Lindberg et al., 2007; Puig et al., 2013) was associated with motor impairment at 6 months, suggesting that integrating structural information could be helpful in predicting behavioral outcome (Feng et al., 2015). Nevertheless, including CST injury percent did not increase the performance of the multivariable models. The modesty of this linkage indicates that functional measures already provide relevant information about structural integrity during the subacute period. In contrast, the role of lesion volume in outcome prediction appears to be more controversial (Saver et al., 1999) (Hayward et al., 2017; Puig et al., 2013; Zaidi et al., 2012).

Combining CST injury and MI connectivity measures predicts motor outcome in subacute stroke (Liu et al., 2015; Rosso et al., 2013). We found that motor recovery can be predicted using fMRI activity estimates alone, with strong model predictive performance. Nevertheless, resting state connectivity estimates do not require any task and remain an interesting alternative strategy to consider as possible biomarkers of stroke recovery.

4.9. Technical considerations and limitations

Some discrepancies between our results and other studies might be explained by the greater stroke severity in our sample, different delays between stroke onset and characterization, different stroke subtypes, or different fMRI methods. First, patients were studied in the context of an ancillary MRI study that was part of stem cell treatment trial, and cell therapy might have affected brain activity patterns. As results of the clinical trial are under analysis, we adjusted the model for the treatment effect by entering treatment as the first covariate. The effect of the other covariates was then introduced stepwise, so that their effects were estimated after cell therapy adjustment. On the other hand, a clinical trial offers the advantage of more standardized clinical practice and therapy including physiotherapy that may vary from one patient to another. Therefore, the use of a stroke sample that was homogeneous in terms of lesion location and mechanism, time of inclusion and follow-up allowed us to minimize intersubject variance. Also, the use of lesion masks in preprocessing, inclusion of head motion estimates and exclusion of motion outliers in the first-level-analysis might have contributed to higher sensitivity in the regional activity estimates. Although the internal validity of our final multivariable model was quite good, external validation using an independent group of stroke patients is the next logical step in this line of research.

5. Conclusion

The current study demonstrates that a passive movement task offers advantages in terms of objectivity, reproducibility and feasibility,

compared to voluntary movement tasks, in studying recovery in patients with moderate to severe stroke (Loubinoux et al., 2001) (Fu et al., 2015; Tombari et al., 2004). Passive movement task-related brain activity measured across the sensorimotor network may provide a set of sensitive and specific biomarkers for assessing and predicting post-stroke motor recovery. Neural reorganization related to motor recovery from moderate to severe stroke results from balanced changes in ipsilesional MI (BA4a) and a set of phylogenetically older sensorimotor regions in the ventral sensorimotor trend. OP1 and OP4 processes may complement the ipsilesional dorsal motor cortex in achieving compensatory sensorimotor recovery. Use of this type of sensorimotor network model is expected to facilitate future clinical research measuring stroke recovery, using it as either a prognostic tool, or a means to measure therapeutic response. Nevertheless, our findings should be generalized with caution to other stroke populations prior to replication of the results in larger studies.

Author contributions

Authors who have contributed to 1) conception and design of the study: Assia Jaillard, Olivier Detante and Marc Hommel, 2) acquisition and analysis of data: Firdaus Fabrice Hannanu, Assia Jaillard, Laurent Lamalle, Antoine Thuriot, Olivier Heck, Olivier Detante and Marc Hommel, and Thomas Zeffiro or 3) drafting a significant portion of the manuscript or figures: Firdaus Fabrice Hannanu, Assia Jaillard and Thomas Zeffiro.

Funding

This work was supported by national grant of PHRC 2007 ISIS (NCT00875654) and 2010 HERMES University Hospital of Grenoble France, and Erasmus + scholarships from European Commission (EACEA) within the BioHealth Computing Master Course.

Disclosures

None.

Acknowledgments

IRMaGe MRI facility was partly funded by the French program “Investissement d'Avenir” run by the “Agence Nationale pour la Recherche”; grant “Infrastructure d'avenir en Biologie Santé” - ANR-11-INBS-0006.

The Clinical Investigation Center (CIC) INSERM UMS 002 CHU Grenoble Alpes has performed data monitoring.

Appendix A. Supplementary data

Supplementary data to this article can be found online at http://dx.doi.org/10.1016/j.nicl.2017.01.023.

References

Agnew, J.A., Zeffiro, T.A., Eden, G.F., 2004. Left hemisphere specialization for the control of voluntary movement rate. NeuroImage 22, 289–303.
Auriat, A.M., et al., 2015. A review of transcranial magnetic stimulation and multimodal neuroimaging to characterize post-stroke neuroplasticity. Front. Neurol. 6, 226.
Bhatt, M.B., et al., 2016. Computational modelling of movement-related beta-oscillatory dynamics in human motor cortex. NeuroImage 133, 224–232.
Blatow, M., et al., 2011. Clinical functional MRI of sensorimotor cortex using passive motor and sensory stimulation at 3 tesla. J. Magn. Reson. Imaging 34, 429–437.
Bradnam, L.V., et al., 2012. Contralesional hemisphere control of the proximal paretic upper limb following stroke. Cereb. Cortex 22, 2662–2671.
Brott, T., et al., 1989. Measurements of acute cerebral infarction: a clinical examination scale. Stroke 20, 864–870.
Burke Quinlan, E., et al., 2015. Neural function, injury, and stroke subtype predict treatment gains after stroke. Ann. Neurol. 77, 132–145.
Burke, E., et al., 2014. Predictors and biomarkers of treatment gains in a clinical stroke trial targeting the lower extremity. Stroke 45, 2379–2384.
Cadoret, G., Smith, A.M., 1997. Comparison of the neuronal activity in the SMA and the ventral cingulate cortex during prehension in the monkey. J. Neurophysiol. 77, 153–166.
Calautti, C., et al., 2007. The relationship between motor deficit and hemisphere activation balance after stroke: a 3 T fMRI study. NeuroImage 34, 322–331.
Carey, L.M., et al., 2005. Motor impairment and recovery in the upper limb after stroke: behavioral and neuroanatomical correlates. Stroke 36, 625–629.
Carey, L.M., et al., 2006. Evolution of brain activation with good and poor motor recovery after stroke. Neurorehabil. Neural Repair 20, 24–41.
Cramer, S.C., et al., 2007. Predicting functional gains in a stroke trial. Stroke 38, 2108–2114.
Doyon, J., Penhune, V., Ungerleider, L.G., 2003. Distinct contribution of the cortico-striatal and cortico-cerebellar systems to motor skill learning. Neuropsychologia 41, 252–262.
Doyon, J., et al., 2009. Contributions of the basal ganglia and functionally related brain structures to motor learning. Behav. Brain Res. 199, 61–75.
Eickhoff, S.B., et al., 2007. The somatotopic organization of cytoarchitectonic areas on the human parietal operculum. Cereb. Cortex 17, 1800–1811.
Eickhoff, S.B., et al., 2010. Anatomical and functional connectivity of cytoarchitectonic areas within the human parietal operculum. J. Neurosci. 30, 6409–6421.
Favre, I., et al., 2014. Upper limb recovery after stroke is associated with ipsilesional primary motor cortical activity: a meta-analysis. Stroke 45, 1077–1083.
Feng, W., et al., 2015. Corticospinal tract lesion load: an imaging biomarker for stroke motor outcomes. Ann. Neurol. 78, 860–870.
Fu, Y., et al., 2015. Comparative functional MRI study to assess brain activation upon active and passive finger movements in patients with cerebral infarction. Eur. Neurol. 73, 13–19.
Gountouna, V.E., et al., 2010. Functional magnetic resonance imaging (fMRI) reproducibility and variance components across visits and scanning sites with a finger tapping task. NeuroImage 49, 552–560.
Hayward, K.S., et al., 2017. Are we armed with the right data? Pooled individual data review of biomarkers in people with severe upper limb impairment after stroke. Neuroimage Clin. 13, 310–319.
Jaillard, A., et al., 2005. Vicarious function within the human primary motor cortex? A longitudinal fMRI stroke study. Brain 128, 1122–1138.
Jang, S.H., et al., 2004. The predictive value of cortical activation by passive movement for motor recovery in stroke patients. Restor. Neurol. Neurosci. 22, 59–63.
Johansen-Berg, H., et al., 2002. The role of ipsilateral premotor cortex in hand movement after stroke. Proc. Natl. Acad. Sci. U. S. A. 99, 14518–14523.
Kantak, S.S., et al., 2012. Rewiring the brain: potential role of the premotor cortex in motor control, learning, and recovery of function following brain injury. Neurorehabil. Neural Repair 26, 282–292.
Kristo, G., et al., 2014. Task and task-free FMRI reproducibility comparison for motor network identification. Hum. Brain Mapp. 35, 340–352.
Kuhn, M.J., et al., 1989. Wallerian degeneration after cerebral infarction: evaluation with sequential MR imaging. Radiology 172, 179–182.
Kutner, M.H., Nachtsheim, C.J., Neter, J., 2004. Applied Linear Regression Models (Vol.).
Lin, F.H., et al., 2009. Functional and effective connectivity of visuomotor control systems demonstrated using generalized partial least squares and structural equation modeling. Hum. Brain Mapp. 30, 2232–2251.
Lindberg, P.G., et al., 2007. Wallerian degeneration of the corticofugal tracts in chronic stroke: a pilot study relating diffusion tensor imaging, transcranial magnetic stimulation, and hand function. Neurorehabil. Neural Repair 21, 551–560.
Lindberg, P.G., et al., 2009. Cortical activity in relation to velocity dependent movement resistance in the flexor muscles of the hand after stroke. Neurorehabil. Neural Repair 23, 800–810.
Liu, J., et al., 2015. Enhanced interhemispheric functional connectivity compensates for anatomical connection damages in subcortical stroke. Stroke 46, 1045–1051.
Loubinoux, I., et al., 2001. Within-session and between-session reproducibility of cerebral sensorimotor activation: a test–retest effect evidenced with functional magnetic resonance imaging. J. Cereb. Blood Flow Metab. 21, 592–607.
Loubinoux, I., et al., 2003. Correlation between cerebral reorganization and motor recovery after subcortical infarcts. NeuroImage 20, 2166–2180.
Loubinoux, I., et al., 2007. Prognostic value of FMRI in recovery of hand function in subcortical stroke patients. Cereb. Cortex 17, 2980–2987.
Mahoney, F.I., Barthel, D.W., 1965. Functional evaluation: the Barthel index. Md State Med J. 14, 61–65.
Marshall, R.S., et al., 2000. Evolution of cortical activation during recovery from corticospinal tract infarction. Stroke 31, 656–661.
Marshall, R.S., et al., 2009. Early imaging correlates of subsequent motor recovery after stroke. Ann. Neurol. 65, 596–602.
Pandya, D.N., 2015. Cerebral Cortex: Architecture, Connections, and the Dual Origin Concept. (Vol.). Oxford University Press.
Puig, J., et al., 2013. Decreased corticospinal tract fractional anisotropy predicts long-term motor outcome after stroke. Stroke 44, 2016–2018.
Quiton, R.L., et al., 2014. Intersession reliability of fMRI activation for heat pain and motor tasks. Neuroimage Clin. 5, 309–321.
Rankin, J., 1957. Cerebral vascular accidents in patients over the age of 60. I. General considerations. Scott. Med. J. 2, 127–136.
Rapin, I., Tourk, L.M., Costa, L.D., 1966. Evaluation of the Purdue Pegboard as a screening test for brain damage. Dev. Med. Child Neurol. 8, 45–54.
Rehme, A.K., et al., 2011. The role of the contralesional motor cortex for motor recovery in the early days after stroke assessed with longitudinal FMRI. Cereb. Cortex 21, 756–768.
Rehme, A.K., et al., 2012. Activation likelihood estimation meta-analysis of motor-related neural activity after stroke. NeuroImage 59, 2771–2782.

Rehme, A.K., et al., 2015. Individual prediction of chronic motor outcome in the acute post-stroke stage: behavioral parameters versus functional imaging. Hum. Brain Mapp.
Rosso, C., et al., 2013. Contribution of corticospinal tract and functional connectivity in hand motor impairment after stroke. PLoS One 8, e73164.
Saver, J.L., et al., 1999. Infarct volume as a surrogate or auxiliary outcome measure in ischemic stroke clinical trials. The RANTTAS Investigators. Stroke 30, 293–298.
Small, S.L., et al., 2002. Cerebellar hemispheric activation ipsilateral to the paretic hand correlates with functional recovery after stroke. Brain 125, 1544–1557.
Steyerberg, E.W., et al., 2001. Internal validation of predictive models: efficiency of some procedures for logistic regression analysis. J. Clin. Epidemiol. 54, 774–781.
Sullivan, K.J., et al., 2011. Fugl-Meyer assessment of sensorimotor function after stroke: standardized training procedure for clinical practice and clinical trials. Stroke 42, 427–432.
Sun, L., et al., 2013. Cortical reorganization after motor imagery training in chronic stroke patients with severe motor impairment: a longitudinal fMRI study. Neuroradiology 55, 913–925.
Tombari, D., et al., 2004. A longitudinal fMRI study: in recovering and then in clinically stable sub-cortical stroke patients. NeuroImage 23, 827–839.
Tzourio-Mazoyer, N., et al., 2002. Automated anatomical labeling of activations in SPM using a macroscopic anatomical parcellation of the MNI MRI single-subject brain. NeuroImage 15, 273–289.
Vogt, B.A., Vogt, L., 2003. Cytology of human dorsal midcingulate and supplementary motor cortices. J. Chem. Neuroanat. 26, 301–309.
Wang, L.E., et al., 2011. Noradrenergic enhancement improves motor network connectivity in stroke patients. Ann. Neurol. 69, 375–388.
Ward, N.S., et al., 2003. Neural correlates of motor recovery after stroke: a longitudinal fMRI study. Brain 126, 2476–2496.
Ward, N.S., et al., 2006. Motor system activation after subcortical stroke depends on corticospinal system integrity. Brain 129, 809–819.
Weiller, C., et al., 1996. Brain representation of active and passive movements. NeuroImage 4, 105–110.
Werhahn, K.J., et al., 2003. Contribution of the ipsilateral motor cortex to recovery after chronic stroke. Ann. Neurol. 54, 464–472.
Wiest, R., et al., 2014. Interhemispheric cerebral blood flow balance during recovery of motor hand function after ischemic stroke—a longitudinal MRI study using arterial spin labeling perfusion. PLoS One 9.
Woosley, C.N., 1958. Organization of somatic sensory and motor areas of the cerebral cortex. In: Harlow, H.F., Woosley, C.N. (Eds.), Biological and Biochemical Bases of Behavior. University of Wisconsin Press, Madison, pp. 63–81.
Zaidi, S.F., et al., 2012. Final infarct volume is a stronger predictor of outcome than recanalization in patients with proximal middle cerebral artery occlusion treated with endovascular therapy. Stroke 43, 3238–3244.